Activation of Camptothecin Derivatives by Conjugation to Triple Helix-Forming Oligonucleotides†

Paola B. Arimondo,*,‡ Gary S. Laco,§ Craig J. Thomas,|| Ludovic Halby,‡ Didier Pez,⊥ Philippe Schmitt,⊥ Alexandre Boutorine,‡ Thérèse Garestier,‡ Yves Pommier,§ Sidney M. Hecht,|| Jian-Sheng Sun,‡ and Christian Bailly#

Laboratoire de Biophysique, CNRS UMR 5153, Muséum National d'Histoire Naturelle, USM0503, INSERM UR565, 43 rue Cuvier, 75231 Paris Cedex 05, France, Laboratory of Molecular Pharmacology, Center for Cancer Research, National Cancer Institute, National Institutes of Health, Bethesda, Maryland 20892-4255, Departments of Chemistry and Biology, University of Virginia, McCormick Road, Post Office Box 400319, Charlottesville, Virginia 22901, Urogene SA, Genopole 4 rue Pierre Fontaine Evry 91000, France, INSERM, U524, IRCL Place Verdun, 59045 Lille, France

Received September 13, 2004; Revised Manuscript Received December 22, 2004

ABSTRACT: Topoisomerase I (topo I) is a ubiquitous DNA-cleaving enzyme and an important therapeutic target in cancer chemotherapy. Camptothecins (CPTs) reversibly trap topo I in covalent complex with DNA but exhibit limited sequence preference. The utilization of conjugates such as triplex-forming oligonucleotides (TFOs) to target a medicinal agent (like CPT) to a specific genetic sequence and orientation within the DNA has been accomplished successfully. In this study, different attachment points of the TFO to CPT (including positions 7, 9, 10, and 12) were investigated and our findings confirmed and extended previous conclusions. Interestingly, the conjugates induced specific DNA cleavage by topo I at the triplex site even when poorly active or inactive CPT derivatives were used. This suggests that the positioning of the drug in the cleavage complex by the sequence-specific DNA ligand is able to stabilize the ternary complex, even when important interactions between topo I and CPT are disrupted. Finally, certain TFO−CPT conjugates were able to induce sequence-specific DNA cleavage with the topo I mutants R364H and N722S that are resistant to camptothecin. The TFO−CPT conjugates are thus valuable tools to study the interactions involved in the formation of the ternary complex and also to enlarge the family of compounds that poison topo I. The fact that an inactive CPT analogue can act as a topo I poison when appropriately coupled to a TFO provides a new perspective at the level of drug design.

Topoisomerase I (topo I)[1] is a ubiquitous DNA-cleaving enzyme and an important therapeutic target in cancer chemotherapy (*1*). Camptothecins (CPTs) trap the intermediate DNA/topo I covalent binary complex (cleavage complex), in which the DNA is cut on one strand and covalently bound to the enzyme through a 3′-phosphotyrosyl bond (*2*), inhibiting the religation step of the catalytic cycle. The formed DNA/topo I/drug ternary complexes can eventually collide with the advancing replication forks, generating irreversible double-stranded DNA (dsDNA) cuts leading to cell death (*3*). Two derivatives of CPT, irinotecan and topotecan, are very effective anticancer agents and are currently used in the clinic (*1*). However, continuing efforts seek to increase the efficacy of these agents, reduce their toxicity in patients, and overcome the tumor drug resistance for this class of compounds. A novel and interesting option would be to increase the sequence specificity of the drug that is limited at this time principally to sites that have a +1 guanine and a −1 thymine at the cleavage site for the enzyme (*4*). Targeting, to a specific chosen DNA site, of the poisoning of the enzyme by CPT can be achieved upon covalent linkage of the drug to a DNA sequence-specific ligand such as a minor groove binder (MGB) or a triplex-forming oligonucleotide (TFO) (*5*−*8*). The ligand moiety of the conjugate binds to its specific site, positions the drugs adjacent to this site, and stabilizes topo I-mediated DNA cleavage only there.

The optimized TFO−CPT conjugates not only induce strong and highly sequence-specific DNA cleavage but also show increased resistance to salt-induced reversal (*8*). Thus,

† This work was supported by grants from Ligue Nationale Contre le Cancer and ACI "Molécules et Cibles thérapeutiques" du Ministère de la Recherche (to P.B.A. and C.B.) and from the European Community (Grant INTAS 01-0638) (to A.B.). This work was supported at the University of Virginia by NIH Research Grant CA78415, awarded by the National Cancer Institute.

* To whom correspondence should be addressed: Laboratoire de Biophysique, UMR5153 CNRS-Muséum National d'Histoire Naturelle, USM0503, INSERM UR565, 43 rue Cuvier, 75231 Paris cedex 05, France. Telephone: +33 1 40793859. Fax: +33 1 40793705. E-mail: arimondo@mnhn.fr.

‡ Muséum National d'Histoire Naturelle.

§ National Institutes of Health.

|| University of Virginia.

⊥ Urogene SA.

INSERM.

[1] Abbreviations: TFO, triplex-forming oligonucleotide; MGB, minor groove binder; bp, base pair; •, Watson−Crick base pairing; x, Hoogsteen base pairing; dsDNA, double-stranded DNA; SAR, structure−activity relationship; topo I, topoisomerase I; 7CPT, 7-(2-aminoethyl)-camptothecin; cCPT, 10-carboxymethyloxycamptothecin; 9CPT, 9-(5-aminopentanoyl)aminocamptothecin; 12CPT, 12-(6-aminohexyl)aminocamptothecin; dCPT, 10-carboxymethyloxy-20-deoxycamptothecin; HATU, *O*-(7-azabenzotriazol-1-yl)-*N*,*N*,*N*′,*N*′-tetramethyluronium-hexafluorophosphate; P, 5-propynyl-2′-deoxyuracil; M, 5-methyl-2′-deoxycytidine.

10.1021/bi048031k CCC: $30.25 © 2005 American Chemical Society
Published on Web 02/25/2005

this strategy offers great promise to develop antitumor agents having increased specificity and efficacy. Recently, we have used the conjugates as useful tools to probe the molecular interactions in the ternary DNA/topo I/drug complex and suggested that different conformations may coexist (*9*). To further study this flexibility in the cleavage complex at the active site, CPT derivatives were here attached to the TFO through different positions, including the 7, 9, 10, and 12 positions. According to structure−activity relationships (SARs) (*10*−*12*) and structural studies (*13*−*15*), positions 7, 9, and 10 are easily substituted and face into the major groove of DNA, which makes them ideal for TFO linkage. Furthermore, it is assumed that inactive CPT derivatives make weaker interactions in the ternary complex (*14*, *15*). We thus studied whether the conjugation of an inactive CPT, a 20-deoxyCPT analogue, to the TFO and its consequent stable positioning in the topo I/DNA binary complex by the formation of the triple helix could stabilize the formed CPT/topo I/DNA ternary complex and make an "inactive" CPT derivative active. Furthermore, it has been suggested that point mutations such as R364H, N722S, and D533G result in CPT resistance by removing important interactions that contribute directly to drug binding (*16*, *17*). The positioning of the CPT derivative by the conjugate in the cleavage complex could create new and stable interactions and thus overcome "resistance".

EXPERIMENTAL PROCEDURES

For the cCPT and dCPT derivatives, mass determination was accomplished by electrospray ionization on a Finnigan 3200 Quadrupole mass spectrometer. HPLC purifications were performed upon a Varian Associates HPLC using an Altech Alltima C_{18} reversed-phase column (250 × 10 mm, 5 μm). ^{1}H and ^{13}C NMR spectra were recorded in chloroform-*d*, acetone-d_6, or DMSO-d_6, on a Varian spectrometer (300 MHz). For all oligonucleotides conjugates, mass determination was accomplished by electrospray ionization on a Q-STAR pulsar I (Appleura) and HPLC purifications were performed upon Agilent 1100 using a Xterra reverse-phase C_{18} column (4.6 × 50 mm, 2.5 μm).

10-HydroxyCPT was purchased from Sino Dragon I/E Co. Ltd. 9-(5-Aminopentanoyl)aminocamptothecin (9CPT) and 12-(6-aminohexyl)aminocamptothecin (12CPT) were gifts from Urogene (France). All other chemicals were purchased from Aldrich Chemical Co. All solvents were of analytical grade. All synthetic transformations of CPT were carried out under dry argon or nitrogen.

MGB hexa(*N*-methylpyrrole)carboxamide was obtained as previously described (*6*).

*Ethyl 10-CarboxymethyloxyCPT (**2**).* To a solution of 10-hydroxyCPT (**1**) (70 mg, 0.19 mmol) in dry acetone (40 mL) was added potassium carbonate (anhydrous) (29 mg, 0.21 mmol), and the mixture was allowed to stir for a 10 min period. To this mixture was added ethyl bromoacetate (35 mg, 0.21 mmol), and the resulting solution was stirred at reflux for an 8 h period. The solvent was removed under diminished pressure, and the resulting colorless was purified by silica-gel column chromatography (95:5 CH_2Cl_2/MeOH) to yield CPT ester **2** as a colorless solid: yield, 53 mg (60%); silica gel TLC R_f, 0.51 (95:5 CH_2Cl_2/MeOH); ^{1}H NMR (DMSO-d_6) δ 0.89 (t, 3H), 1.24 (t, 3H), 1.88 (m, 2H), 4.21 (q, 2H), 5.01 (s, 2H), 5.28 (s, 2H), 5.43 (s, 2H), 6.52 (s, 1H), 7.31 (s, 1H), 7.55 (m, 2H), 8.11 (d, 1H), 8.57 (s, 1H); mass spectrum (FAB), *m*/*z* 451.1505 $(M + H)^+$ ($C_{24}H_{23}N_2O_7$ requires 451.1505).

*Ethyl 10-Carboxymethyloxy-20-chloroCPT (**3**).* To a solution of CPT ester **2** (50 mg, 0.11 mmol) in freshly distilled benzene (25 mL) was added pyridine (90 μL, 1.1 mmol), and the resulting solution was allowed to stir for a 5 min period. To this solution was added thionyl chloride (41 μL, 0.47 mmol), and the resulting solution was allowed to stir at reflux for a 2 h period. The solvent was removed under diminished pressure, and the resulting solid was purified by silica-gel column chromatography (95:5 CH_2Cl_2/MeOH) to yield 20-chloroCPT ester **3** as a yellow solid: yield, 51 mg (98%); silica-gel TLC R_f, 0.54 (95:5 CH_2Cl_2/MeOH).

*Ethyl 10-Carboxymethyloxy-20deoxyCPT (**4**).* To a solution of 20-chloroCPT ester **3** (51 mg, 0.11 mmol) in methanol (20 mL) in the presence of palladium on carbon (10%) (10 mg) was maintained under hydrogen gas (20 psi) for 6 h. The catalyst was removed by filtration, and the solvent was concentrated under diminished pressure. The resulting solid was purified by silica-gel column chromatography (95:5 CH_2Cl_2/MeOH) to yield deoxyCPT ester **4** as a colorless solid: yield, 20 mg (42%); silica-gel TLC R_f, 0.53 (95:5 CH_2Cl_2/MeOH); ^{1}H NMR (DMSO-d_6) δ 1.00 (t, 3H), 1.26 (t, 3H), 2.01 (m, 2H), 3.82 (t, 1H), 4.22 (q, 2H), 4.98 (s, 2H), 5.21 (s, 2H), 5.38 (m, 2H), 7.14 (s, 1H), 7.32 (m, 2H), 8.05 (d, 1H), 8.49 (s, 1H); mass spectrum (FAB), *m*/*z* 435.1540 $(M + H)^+$ ($C_{24}H_{23}N_2O_6$ requires 435.1556).

*10-Carboxymethyloxy-20-deoxyCPT (**5**) or dCPT.* To a solution of deoxyCPT ester **4** (24 mg, 0.06 mmol) in ethanol (10 mL) and water (10 mL) at 0 °C was added potassium carbonate (7 mg, 0.05 mmol), and the resulting solution was stirred for a 4 h period, while the reaction was monitored by TLC. The solvent was concentrated under diminished pressure, and the resulting solid was dissolved in 15 mL of water at 0 °C. Purification was achieved by reversed-phase HPLC using a linear gradient of 0.1% trifluoroacetic acid in water containing increasing amounts of acetonitrile (0 → 25 min, linear gradient from 24 to 39% at a flow rate of 4 mL/min; t_R, 17.4 min) to yield deoxyCPT acid **5** as a colorless solid: yield, 17 mg (76%); ^{1}H NMR (DMSO-d_6) δ 0.99 (t, 3H), 2.01 (m, 2H), 3.81 (t, 1H), 4.91 (s, 2H), 5.24 (s, 2H), 5.39 (m, 2H), 7.18 (s, 1H), 7.52 (m, 2H), 8.07 (d, J = 8.3 Hz, 1H), 8.52 (s, 1H); mass spectrum (FAB), *m*/*z* 429.1062 $(M + Na)^+$ ($C_{22}H_{18}N_2O_6Na$ requires 429.1063).

10-CarboxymethyloxyCPT or cCPT. To a solution of CPT ester **2** (40 mg, 0.09 mmol) in ethanol (10 mL) and water (10 mL) at 0 °C was added potassium carbonate (12 mg, 0.9 mmol), and the resulting solution was stirred for a 4 h period, while the reaction was monitored by TLC. The solvent was removed under diminished pressure, and the resulting solid was dissolved in 15 mL of water at 0 °C. Purification was achieved by reversed-phase HPLC using a linear gradient of 0.1% trifluoroacetic acid in water containing increasing amounts of acetonitrile (0 → 25 min, linear gradient from 24 to 39% at a flow rate of 4 mL/min; t_R, 12.4 min) to yield cCPT as a colorless solid: yield, 12 mg (31%); ^{1}H NMR (DMSO-d_6) δ 0.90 (t, 3H), 1.91 (m, 2H), 4.90 (s, 2H), 5.28 (s, 2H), 5.43 (m, 2H), 7.31 (s, 1H), 7.52 (m, 2H), 8.12 (d, J = 8.3 Hz, 1H), 8.59 (s, 1H); mass

spectrum (FAB), *m*/*z* 445.1011 $(M + Na)^+$ ($C_{22}H_{18}N_2O_7Na$ requires 445.1012).

CPT Analogues. All of the CPT analogues were dissolved in DMSO at 5 mM and then diluted further with water prior to use. The final DMSO concentration never exceeded 0.3% (v/v) in all assays. They were attached to the 3′ end of the TFO as described in Figure 2.

Oligonucleotides. Oligonucleotides were purchased from Eurogentec (Belgium) and purified using quick spin Sephadex G-25 (BioRad). Concentrations were determined spectrophotometrically at 25 °C using molar extinction coefficients at 260 nm calculated from a nearest-neighbor model (*18*).

The nomenclature of the oligonucleotides and conjugates is the following: the abbreviation TFO is followed by a number referring to the length of the oligonucleoide, followed by the letter L (for linker), the number of carbon atoms in the linker, and finally, by the denomination of the CPT analogue [cCPT for 10-carboxymethyloxycamptothecin, 7CPT for 7-(2-aminoethyl)camptothecin, dCPT for the 10-carboxymethyloxy-20-deoxycamptothecin, 9CPT for 9-(5-aminopentanoyl)aminocamptothecin, and 12CPT for 12-(6-aminohexyl)aminocamptothecin].

Synthesis of the Conjugates. The CPT derivatives were conjugated to the terminal amino group of different linker arms at the 3′ of the oligonucleotide according to the procedures previously described (*6*, *8*, *19*) or as following.

Synthesis of TFO16−L4−cCPT and TFO16−L4−dCPT. A total of 310 μg (60 nmol) of 3′-phosphorylated oligonucleotide TFO was precipitated as the hexadecyltrimethylammonium salt and was then dissolved in 50 μL of dry DMSO. Solutions of 4-(dimethylamino)pyridine (5 mg in 25 μL of DMSO, 41 μmol), dipyridyl disulfide (6.6 mg in 25 μL of DMSO, 30 μmol), and triphenylphospine (7.9 mg in 50 μL of DMSO, 30 μmol) were added. After 15 min of incubation at room temperature, 1,4-diaminobutane (5 mg, 57 μmol) was added to the activated oligonucleotide. The mixture was kept for 2 h at room temperature. The oligonucleotide derivative was then precipitated with 2% $LiClO_4$ in acetone, rinsed with acetone, and dissolved in 50 μL of water. The attachment of the diamino linker was quantitative. Then, dCPT or cCPT was attached by activating the carboxyl group with *O*-(7-azabenzotriazol-1-yl)-*N*,*N*,*N*′,*N*′-tetramethyluroniumhexafluorophosphate (HATU). The oligonucleotide derivative was precipitated as the hexadecyltrimethylammonium salt and dissolved in 100 μL of dry DMSO. dCPT or cCPT (400 μg, 1 μmol), HATU (380 μg, 1.1 μmol), and 1 μL of triethylamine were added. The reaction was kept at room temperature for 4 h. The oligonucleotide conjugate was then precipitated with 2% $LiClO_4$ in acetone, rinsed with acetone, and purified by reversed-phase HPLC using a linear acetonitrile gradient [0 → 80% CH_3CN in 0.2 M (NH_4)OAc]. The average yield was 40%. The oligonucleotide conjugates were characterized by UV spectroscopy, denaturing gel electrophoresis, and mass spectrometry. TFO16−L4−cCPT MS (ES^-) *m*/*z* 5618 $[M - H]^-$ (calculated, 5617); TFO16−L4−dCPT MS (ES^-) *m*/*z* 5602 $[M - H]^-$ (calculated, 5602).

Because it is known that 20-deoxyCPT can be oxidized by O_2 to afford CPT itself, for the assays, the conjugates were dissolved in water just prior to utilization.

Synthesis of TFO16−9CPT and TFO16−12CPT. A sample of 310 μg (60 nmol) of 3′-phosphorylated oligonucleotide was precipitated as the hexadecyltrimethylammonium salt and dissolved in 50 μL of dry DMSO. Solutions of 4-(dimethylamino)pyridine (5 mg in 25 μL of DMSO, 41 μmol), dipyridyl disulfide (6.6 mg in 25 μL of DMSO, 30 μmol) and triphenylphospine (7.9 mg in 50 μL of DMSO, 30 μmol) were added. After 15 min of incubation at room temperature, CPT derivative 9CPT or 12CPT (0.4 mg, 1 μmol) was added to the activated oligonucleotide. The mixture was kept at room temperature for 4 h. The oligonucleotide conjugate was precipitate from the mixture by the addition of 2% $LiClO_4$ in acetone, rinsed with acetone, and purified by reversed-phase HPLC using a linear acetonitrile gradient [0 → 80% CH_3CN in 0.2 M (NH_4)OAc]. The average yield was 40%. The oligonucleotide conjugates were characterized by UV spectroscopy and denaturing gel electrophoresis. TFO16−9CPT MS (ES^-) *m*/*z* 5603 $[M - H]^-$ (calculated, 5603).

Synthesis of MGB Conjugates. dCPT and cCPT were attached to the MGB hexa(*N*-methylpyrrole)carboxamide according to the procedure previously described (*6*). MGB−dCPT MS (ES^-) *m*/*z* 1393 $[M - H]^-$ (calculated, 1392); MGB−cCPT MS (ES^-) *m*/*z* 1409 $[M - H]^-$ (calculated, 1408).

DNA Fragment. The plasmid pBSK(±) was purchased from Promega (France), and the 77 base pair (bp) target duplex was inserted between the *Bam*HI and *Eco*RI sites (Figure 2 for the sequence). The detailed procedures for isolation, purification, and labeling of a 324-bp DNA fragment have been described previously (*8*).

Topo I and Mutants. Recombinant human topo I (topo I wild type), mutant topo I R364H, and mutant topo I N722S were purified from TN5 insect cells using a Baculovirus construct for the NH_2-terminus-truncated human topo I cDNA as described previously (*14*, *20*).

Topo I Cleavage Assays. The 324-bp radiolabeled target duplex (50 nM) was incubated at 30 °C for 90 min, in 50 mM Tris-HCl at pH 7.2, containing 60 mM KCl, 10 mM $MgCl_2$, 0.5 mM DTT, 0.1 mM EDTA, and 30 μg/μL BSA, in the presence of the TFO or MGB, at the indicated concentration (total reaction volume of 10 μL). The DNA−topo I cleavage complexes were dissociated by the addition of SDS (final concentration of 0.5%). After ethanol precipitation, all samples were resuspended in 6 μL of formamide, heated at 90 °C for 4 min, and then chilled on ice for 4 min, before being loaded onto a denaturing 8% polyacrylamide gel (19:1 acrylamide/bisacrylamide) containing 7.5 M urea in 1×TBE buffer (50 mM Tris base, 55 mM boric acid, and 1 mM EDTA). To quantitate the extent of cleavage, the gels were scanned with a Typhoon 9410 (Amersham Biosciences). For the determination of cleavage levels, normalization relative to the total loading was performed. The cleavage efficacy was also normalized for each drug to the cleavage efficacy of topo I alone in each experiment. The experiments were repeated between 4 and 10 times.

Molecular Modeling. The X-ray crystal structure of human topo I in covalent complex with DNA (*21*) was previously prepared for molecular modeling as described (*22*). The solvated and electroneutral topo I/DNA complex with a docked CPT was then further modified in the following ways using Insight II version 2000.1 molecular-modeling software

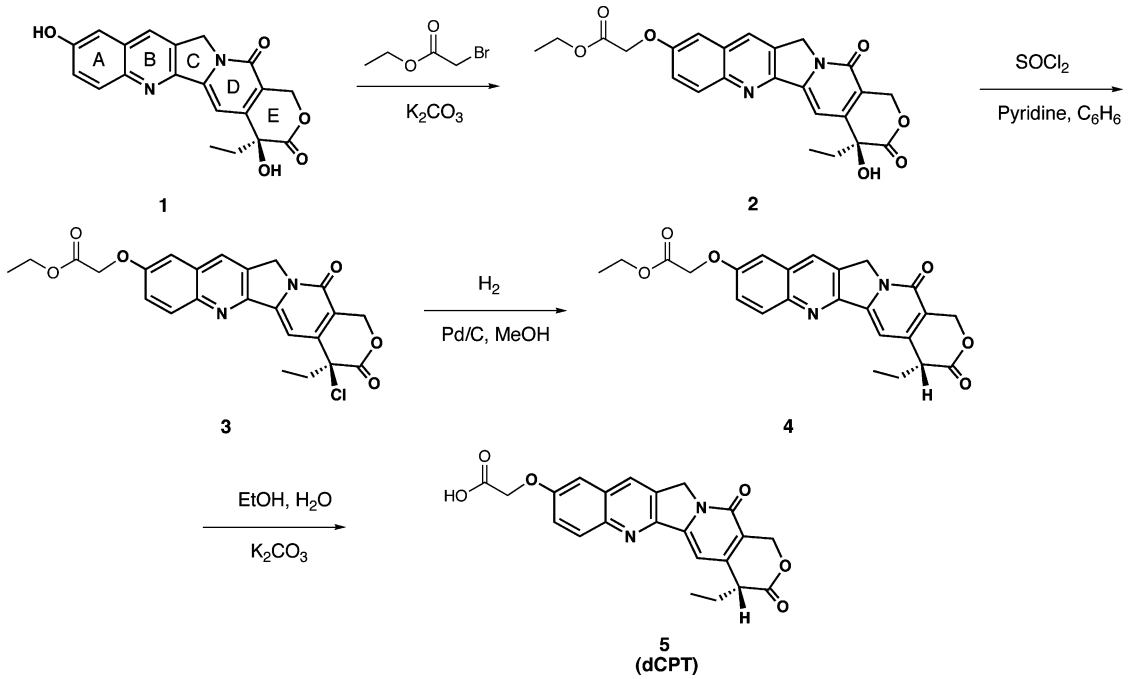

FIGURE 1: Synthetic route used for the preparation of 20-deoxy-10-carboxymethyloxycamptothecin dCPT.

(Accelrys, San Diego, CA): (1) The +1 through +4 bases, relative to the cleavage site, of both DNA strands were replaced with the corresponding bases used in this study, and the remaining deoxynucleosides greater than +4 were deleted. (2) A B-form triple-helix DNA was then added to the model. The triple helix is composed of B-form A and T homopolymer strands with a TFO annealed to the nonscissile A strand. The triple-helix A and T homopolymer strands' backbones were bound to the corresponding backbones of the +4 nonscissile- and scissile-strand deoxynucleosides. The bonds were then minimized in Insight II/Discover_3 using the CFF force field to a final convergence of 1. (3) The indicated linkers were built in Insight II/Biopolymer and then bonded to the 3′-O of the TFO. (4) The indicated CPT derivative was then bonded to the linker at the indicated position (see Figure 2). (5) The topo 1/triple helix/CPT complex was then resolvated, and additional sodium atoms were added to the backbone phosphates of the triple helix to keep the system electroneutral. The linker CPT as well as active-site residues (excluding Tyr723), surrounding bases including the rotated +1 deoxynucleoside, water, and ions within 20 Å were minimized to a final convergence of 1 with no restraints. Note: the CFF force field lacks a torsion parameter for the P−N bond found in all linkers. As a result, the torsion stop control was turned off prior to the minimization. (6) For interaction energy scores calculations, water, ions, and DNA were first merged with topo I. The interaction energy scores between the indicated CPT and topo I/DNA were calculated in Insight II/Docking with a 20 Å cutoff. The TFO and linker were not included in the interaction energy score calculation.

RESULTS

Synthesis of the CPT Analogues. To test the attachment point of CPT to the TFO, we used 9CPT and 12CPT, bearing suitable linker arms in positions 9 and 12, respectively.

Synthetic elaboration of a CPT derivative with a carboxymethyloxy linker at C_{10} of the quinoline ring of CPT has been previously reported (*7*, *9*). Further, the removal of the 20-hydroxyl group results in an inactive derivative and has been reported previously and utilized in numerous studies (*11*, *23*, *24*). The goal of this experiment was to prepare a CPT analogue containing both features, required for the preparation of the TFO−CPT conjugate of a CPT derivative known not to form a stable ternary complex with topo I and DNA. It is also important to note that C20-deoxyCPT analogues are liable to reoxidize under relatively mild conditions, thus necessitating that transformations utilizing reagents or conditions capable of 20 oxygenation should be avoided (ref *24* and references therein). Accordingly, a straightforward four-step semisynthetic procedure starting with 10-hydroxylCPT was used (Figure 1).

Treatment of **1** with ethyl bromoacetate and anhydrous K_2CO_3 in refluxing acetone produced ester **2** in 60% yield. The ester was then heated at reflux with 4 equiv of thionyl chloride in the presence of 10 equiv of pyridine in anhydrous benzene for 4 h. After purification, the resulting chloride **3** was reduced using hydrogen gas over Pd/C (10%) to yield the 20-deoxyCPT ester **4** in 42% yield for two steps. Saponification of deoxy ester **4** via treatment with K_2CO_3 in a 1:1 mixture of ethanol and water resulted in the formation of the 20-deoxy CPT acid **5** (dCPT) in 76% yield.

Synthetic production of cCPT was performed in a manner similar to that previously reported (*7*, *9*).

Given the natural tendency of the C_{20} position to reoxidize, a mock coupling reaction was performed to determine the stability of the 20-deoxy species toward the conditions needed to synthesize the TFO conjugates. Utilizing 4-aminobutanol as a model amine, the 20-deoxy CPT derivative **4** was coupled using BOP and diisopropylethylamine to produce the amide conjugate. Low-resolution mass spectrometry demonstrated that the C_{20} position remained unoxidized through the synthesis and purification of this model conjugate (data not shown).

Conjugates. The target DNA sequence used in this study and the newly synthesized TFO−CPT are shown in Figure

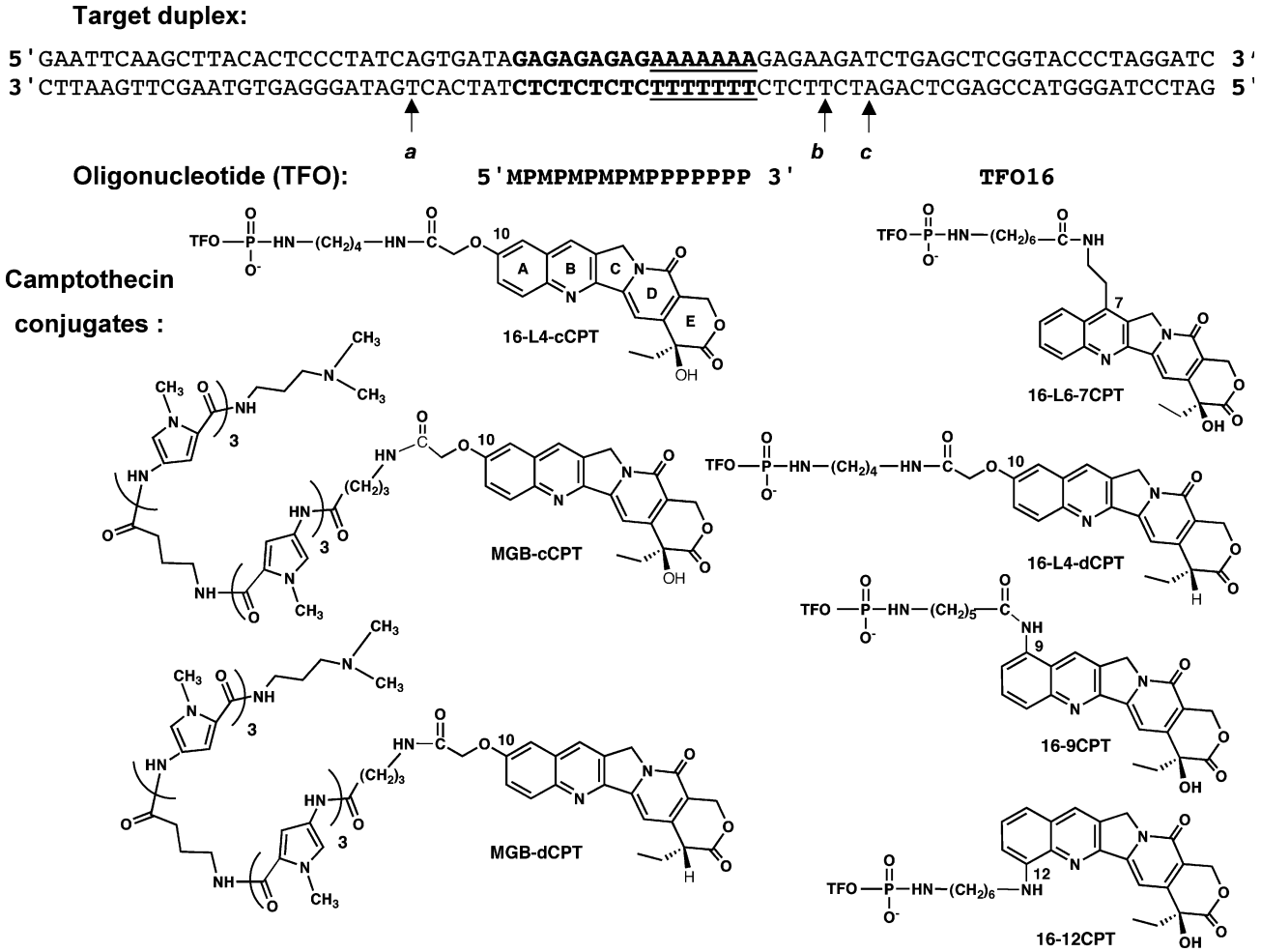

FIGURE 2: Sequence of the target and TFO used in this study and the structure of the conjugates. The 16-bp triplex target site is shown in bold. The binding site of the MGB is underlined. The TFO binds in the major groove in a parallel orientation to the oligopurine strand of the duplex. The 77-bp duplex target was inserted between the *Bam*HI ad *Eco*RI sites of pBS(±). The CPT-stabilized topo-I-mediated DNA cleavage sites in the proximity to the triple helix are indicated by arrows (sites a, b, and c). M = 5-methyl-2′-deoxycytidine, and P = 5-propynyl-2′-deoxyuridine. The different CPT derivatives were attached to the 3′ end of the TFO. The TFO is abbreviated with 16-mer in the names of the conjugates for all figures.

2. The oligopurine·oligopyrimidine triplex target site is 24-bp long and is contained in a 77-bp duplex inserted in pBSK-(±) as previously described (*8*). A resulting 324-bp 3′-^{32}P-end-labeled DNA fragment was used for topo-I-mediated DNA cleavage studies. The TFO used is a 16-mer (TFO16) and contains 5-methyldeoxycytosines and 5-propynyldeoxyuracils to form a stable triplex at physiological pH and temperature (*25*). The MGB used is a hairpin polyamide containing two sets of three *N*-methylpyrrole carboxamide units (abbreviated MGB) that we have previously attached to 10-carboxycamptothecin to induce sequence-specific DNA cleavage (*6*).

The TFO and MGB were attached at their 3′ end to position 10 of an active camptothecin (cCPT) or its inactive 20-deoxy derivative (dCPT). In the case of the TFO conjugates, a spacer of 4 carbon atoms (diaminobutane) was used, in agreement with previous findings (*8*). Furthermore, SARs (*11*, *12*) and structural studies (*13*−*15*) have indicated that positions 7, 9, and 10 face into the major groove of the DNA and that bulky substitutions at these positions do not decrease the pharmacological activity, while substitutions in positions 11 and 12 do diminish activity. Because TFO binds in the major groove, positions 7, 9, and 10 seemed quite favorable for the coupling. Having already used positions 7 and 10, we attached to the TFO 9CPT, a CPT derivative containing a linker arm at position 9 with a terminal amino group suitable for conjugation. Attachment to position 12 of CPT was also explored by using 12CPT, bearing a diaminohexyl linker in position 12.

Effect of the Drug Attachment Site. DNA cleavage by topo I in the presence of the 9CPT and 12CPT conjugates is shown in Figure 3. The 324-bp DNA restriction fragment 3′-^{32}P-end labeled on the oligopyrimidine-containing strand of the duplex was incubated in the presence of topo I and either the CPT derivatives alone or linked to the TFO. The new cCPT derivative and its conjugate (TFO16−L4−cCPT) were used as controls and behaved as the previously studied conjugates attached through position 10 (*8*, *9*). In fact, while 5 μM of cCPT (lane 3) stabilized topo-I-mediated DNA cleavage at different sites (a, b, and c), in the presence of the triplex formed by 0.5 μM TFO16−L4−cCPT (lane 4), cleavage increased only at site b, situated 4 bp from the triplex 3′ end, as expected. Noteworthy, throughout this study, the conjugates were used at concentrations 5−10-fold lower than that for CPT, because the tethered molecules are considerably more potent than the free drug at inducing topo-

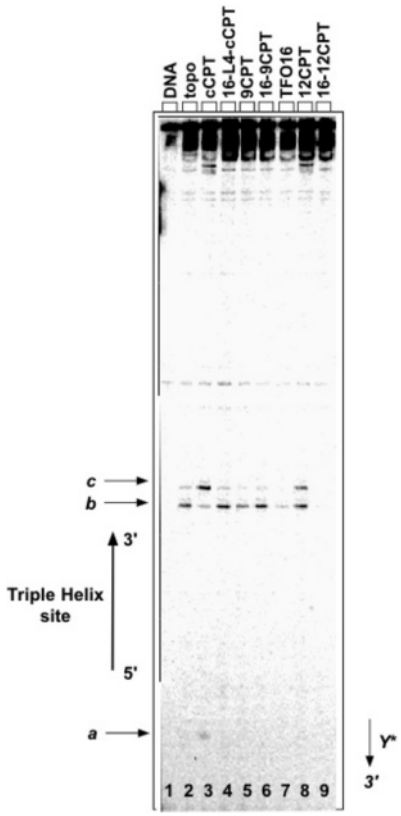

FIGURE 3: Sequence analysis of the topo-I-mediated cleavage products in the presence of the TFO16−9CPT and TFO16−12CPT conjugates. A 324-bp duplex, 3′-^{32}P-end labeled on the oligopyrimidine strand (lane 1) was incubated with topo I (lane 2) in the presence of 5 μM cCPT (lane 3), 0.5 μM TFO16−L4−cCPT (lane 4), 5 μM 9CPT (lane 5), 0.5 μM TFO16−9CPT (lane 6), 0.5 μM TFO16 (lane 7), 5 μM 12CPT (lane 8), or 0.5 μM TFO16−12CPT (lane 9). The positions of the cleavage sites are indicated (sites a−c), as is the region corresponding to the triplex site.

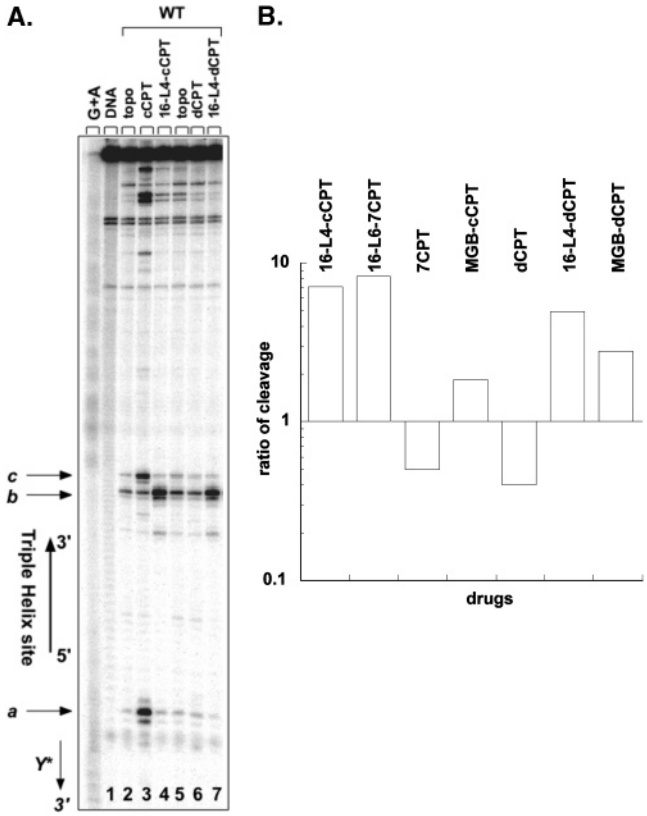

FIGURE 4: Effect of the 20-*S*-hydroxyl group on the cleavage by the TFO−CPT conjugate. (A) 324-bp duplex (lane 1) was incubated with topo I (lane 2) in the presence of 5 μM cCPT (lane 3), 0.5 μM TFO16−L4−cCPT (lane 4), topo I (lane 5), 5 μM dCPT (lane 6), or 0.5 μM TFO16−L4−dCPT (lane 7). Adenine/guanine-specific Maxam−Gilbert chemical cleavage reactions were used as markers. The positions of the cleavage sites are indicated (sites a−c), and the region corresponding to the triplex site is indicated by an arrow. (B) Ratio between the intensity of cleavage at site b in the presence of the triple helices and the intensity in the presence of cCPT alone is represented, on a logarithmic scale, for wild-type topo I. Data were compiled from 10 independent experiments.

I-mediated DNA cleavage (*8*). Under the experimental conditions, all conjugates formed a triplex helix (data not shown). Unexpectedly, the 9CPT derivative was poorly active with a cleavage pattern (lane 5) corresponding to that of topo I alone (lane 2). Upon covalent linkage to the 16-mer TFO (TFO16−9CPT) and triplex formation (lane 6), a sequence-specific DNA cleavage was observed at site b, comparable in intensity to that of TFO16−L4−cCPT (lane 4). The attachment through the unfavorable 12 position abolished the cleavage ability of the conjugate (lane 9), even though 12CPT is an active topo I poison (lane 8). This observation is in agreement with previous SARs that suggested that substitutions in that part of the quinolone moiety of the alkaloide decreases biological activity (*10*−*12*, *26*). The binding of the TFO alone (TFO16) affects only partially topo I cleavage (lane 7).

Activation by Conjugation to TFO of Inactive Topo I Poisons. These preliminary results suggested that upon conjugation to a TFO it is possible to induce a strong sequence-specific DNA cleavage with relatively poor topo I poisons. To test this hypothesis, we used 20-deoxyCPT, which has been shown to be inactive (*11*, *23*, *24*). This analogue was attached through a 10-carboxylmethyloxy group to the diaminobutane linker at the 3′ end of the TFO16 to obtain TFO16−L4−dCPT. Figure 4A shows the analysis of the topo I cleavage products on the radiolabeled target DNA in the presence of the 20-deoxyCPT derivative (dCPT, lane 6) or in the presence of its corresponding conjugate (lane 7). The parent 20-*S*-OH derivatives were used as the control (cCPT, lane 3 and TFO16−L4−cCPT, lane 4). Clearly, the covalent linkage to the TFO and formation of the triple-helical structure enabled the otherwise inactive 20-deoxyCPT to stabilize strong DNA cleavage by topo I at site b (lane 7), comparable to the control conjugate TFO16−L4−cCPT (lane 4). The conjugates are thus able to position this inactive CPT analogue in the cleavage complex and stabilize the ternary complex. In Figure 4B, the ratio of the intensity of cleavage at site b in the presence of the conjugate or another CPT derivative over the intensity in the presence of cCPT is represented on a logarithmic scale. All conjugates induced a sequence-specific DNA cleavage at site b, regardless of which CPT derivative was used. Furthermore, the MGB−dCPT conjugate was also able to induce an efficient sequence-specific cleavage at site b (Figure 4B), indicating that the targeting is equivalent whether the CPT derivative is brought from either the major groove (by the TFO) or the minor groove (by the MGB).

These results imply that the conjugation of normally inactive CPT derivatives to sequence-specific DNA ligands can enable compounds that lack important functional groups

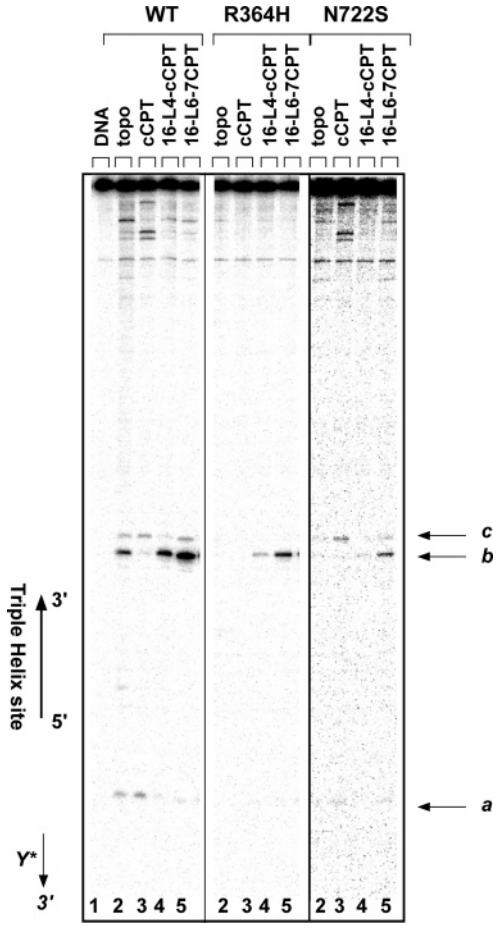

FIGURE 5: Effect of the topo I mutants on the sequence-specific cleavage. A 324-bp duplex (lane 1) was incubated with topo I wild type or mutants R364H or N722S (lane 2) in the presence of 5 μM 10CPT (lane 3), 0.5 μM TFO16−L4−cCPT (lane 4), or 0.5 μM TFO16−L6−7CPT (lane 5). Adenine/guanine-specific Maxam−Gilbert chemical cleavage reactions were used as markers. The positions of the cleavage sites are indicated (sites a−c) as well as the region corresponding to the triplex site.

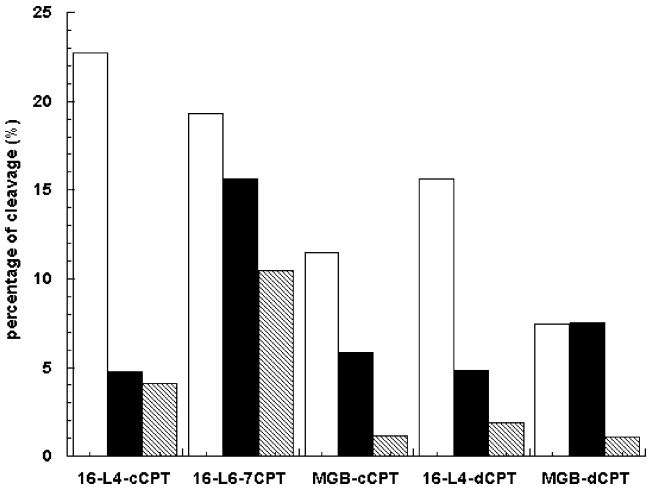

FIGURE 6: Intensity of cleavage of the conjugates in the presence of the three topoisomerases I. The intensity of cleavage at site b in the presence of the conjugates is represented for wild-type topo I (white bars), the R364H mutant (black bars), and the N722S mutant (hatched bars). Data were compiled from 4−10 independent experiments as described in the Experimental Procedures.

Table 1: Loss of DNA Cleavage Activity in the Presence of the Topo I Mutants at Site b[a]

	loss R364H	loss N722S
cCPT	−0.48	−0.61
TFO16−L4−cCPT	−0.58	−0.72
MGB−cCPT	−0.10	−0.50
7CPT	−0.07	−0.52
TFO16−L6−7CPT	+0.16	−0.10
dCPT	−0.10	−0.45
TFO16−L4−dCPT	−0.12	−0.45
MGB−dCPT	−0.01	−0.86

[a] The loss is calculated as −(1 − percentage of cleavage in the presence of the mutant/percentage of cleavage in the presence of the wild type), where the percentage of cleavage is normalized to the percentage of cleavage in the presence of topoisomerase I (wild type or mutants) at site b. The mean value of 3−10 experiments is reported.

for the stabilization of the ternary complex. It is known that CPT resistance results from point mutations in human topo I that, in several cases, disrupt hydrogen bonds stabilizing the CPT binding to the topo I/DNA cleavage complex (*13*−*15*, *24*). The next question was thus to investigate whether the conjugates were able to form a stable ternary complex with topo I mutants that still cleave DNA but are no longer sensitive to CPT poisoning (*14*, *17*, *20*).

Cleavage in the Presence of CPT-Resistant Topo I Mutants. We used two CPT-resistant mutants found in CPT-resistant cancer cell lines: the R364H mutant, in which arginine 364 is replaced by an histidine (*27*), and the N722S mutant, containing a serine instead of asparagine 722 (*28*). Figure 5 shows that the TFO16−L4−cCPT conjugate (lane 4) followed the resistance profile of cCPT alone (lane 3). Interestingly, conjugate TFO16−L6−7CPT, attached to 7-(2-aminoethyl)camptothecin (*8*), induced some sequence-specific cleavage at site b in the presence of the topo I mutants (lanes 5). Figure 6 depicts the percentage of cleavage of several conjugates in the presence of the topo I tested. It clearly appears that conjugate TFO16−L6−7CPT was able to induce cleavage also in the presence of the topo I mutants.

Table 1 summarizes the loss in DNA cleavage at site b in the presence of the topo I mutants for each conjugate compared to the corresponding CPT derivative alone. The percentage of cleavage for each drug, free or conjugated, has been normalized to the amount of basal cleavage observed in the presence of the enzyme alone. For the analysis of the results, it is important to note that the topo I mutants cleave the 324-bp DNA fragment less efficiently than does the wild-type enzyme. TFO16−L4−cCPT is comparable to cCPT, while the MGB conjugate MGB−cCPT was still active with the R364H mutant. 7CPT induced cleavage with the R364H mutant, while in the presence of the N722S mutant, it behaved as cCPT (Figures 5 and 6). The corresponding TFO16−L6−7CPT conjugate trapped topo I/DNA cleavage complexes in the presence of both mutants, showing a very small loss of activity. With the topo I mutants, the 20-deoxy TFO conjugate (TFO16−L4−dCPT) showed a loss of activity comparable to the 20-*S*-OH equivalent, while the MGB conjugate MGB−dCPT still stabilized the cleavage complex in the presence of the R364H but showed a large loss of cleavage activity with the N722S mutant.

Molecular-Modeling Studies. To better understand the results obtained with the 20-deoxy CPT TFO conjugate (TFO16−L4−dCPT) and the topo I mutants, we compared by molecular-modeling studies how the TFO positions the

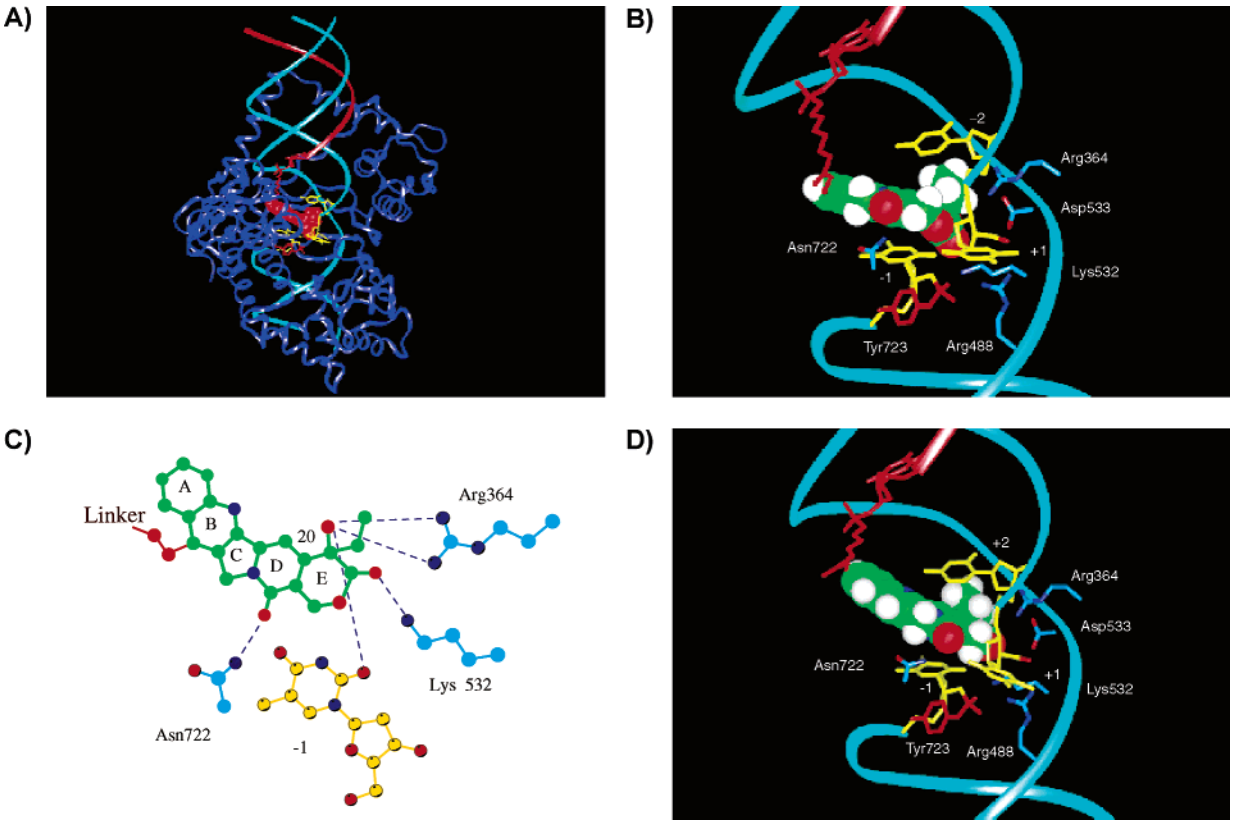

FIGURE 7: Minimized structural models for the topo I/DNA complex in the presence of the conjugates. Topo I backbone in blue ribbon, DNA backbone in teal ribbon, TFO backbone in red ribbon, linker in red, and CPT rendered in CPK. Bases around CPT are in yellow, −1 scissile-strand base below CPT, rotated +1 scissile-strand base to the right of CPT, +1 scissile-strand base above CPT, active-site Tyr723 and tyrosil-phosphate bond to −1 thymine in red. (A) Topo I/DNA in the presence of TFO16−L6−7CPT. (B) Close up of A. (C) Flattened view of B with dashed lines indicating hydrogen-bonds/electrostatic interactions between CPT and the topo 1/DNA active site. (D) Close up of the topo I/DNA complex in the presence of TFO16−L4−cCPT. Selected atom colors: oxygen, red; nitrogen, dark blue; carbon, green; and hydrogen, white.

different CPTs in the topo I/DNA cleavage complex (Figure 7). Accordingly, when CPT is linked at the 7 position to the TFO (TFO16−L6−7CPT), it is able to dock in a planar orientation with respect to the active-site bases (parts A and B of Figure 7), and therefore, to stack with the −1 thymine and make a network of direct hydrogen-bond/electrostatic interactions with the topo I/DNA active site including (Figure 7C): (1) the D-ring carbonyl oxygen hydrogen-bonds to N722, which when mutated results in a CPT-resistant topo I (*28*); (2) the E-ring carbonyl oxygen hydrogen-bonds to K532, an essential residue (*29*); (3) the 20-*S*-OH hydrogen hydrogen-bonds to the −1 scissile-strand thymine carbonyl oxygen; and (4) the 20-*S*-OH oxygen makes an electrostatic interaction with R364, which when mutated results in a resistant topo I (*27*). The fact that the TFO and linker allows CPT to make an optimal orientation in the topo I/DNA active site could explain the cleavage activity of the TFO16−L6−7CPT conjugate in the presence of the two topo I mutants (Figures 5 and 6 and Table 1). In contrast, when the cCPT conjugate is linked at position 10 (TFO16−L4−cCPT), the E-ring carbonyl oxygen makes a rather long hydrogen-bond to K532 at 3.2 Å, the D-ring carbonyl oxygen still makes a hydrogen-bond to N722, while the 20-*S*-OH does not make any hydrogen-bonds and has a significantly weaker electrostatic interaction with R364 (Figure 7D and data not show). These results are due to the attachment to CPT via the A-ring 10 position that prevents cCPT from adopting a planar orientation, with respect to the bases, in the topo I/DNA active site. The fact that the 20-*S*-deoxyCPT (TFO16−L4−dCPT) conjugate has similar activity as 20-*S*-OH TFO16−L4−cCPT is consistent with the 20*S*-OH not making hydrogen-bonds to the topo I/DNA active site when part of these conjugates.

DISCUSSION

According to SARs and structural studies (*10*−*15*, *23*, *26*), positions 7, 9, and 10 are suitable locations for large substituents, without clashing with the surrounding topo I and DNA structures. Furthermore, they face into the major groove, making them ideal for TFO linkage. In agreement with these experimental observations, conjugation of the major-groove-binding TFO to CPT analogues at positions 7, 9, or 10 induced a specific DNA cleavage by topo I at the triplex site. In contrast, positions 11 and 12 are considered unfavorable to bulky substitutions, although some substitutions in position 11, as 10,11-(methylenedioxy), 10,11-(ethylenedioxy), 11-fluoro, and 11-cyano, have resulted in active compounds (*30*, *31*). Conjugation of the TFO to the active 12CPT derivative through a side chain at position 12 gave an inactive conjugate, confirming the previous SAR findings for CPT.

Interestingly, the 9CPT derivative used here was a poor topo I poison, while the corresponding TFO−9CPT conjugate was able to induce DNA cleavage by topo I (Figure 3). To further explore whether the conjugates were able to induce DNA cleavage with inactive CPT analogues, we synthesized

a derivative of the well-characterized inactive CPT derivative, 20-deoxyCPT (*23*, *24*). In fact, the 20-hydroxyl group of the E-ring lactone of CPT is known to be of importance in rendering CPT an active poison of topo I. A primary role of the 20-hydroxyl group seems to be to produce a specific interaction within the DNA/topo I cleavage complex (Figure 7C). In the recent crystal structure of the ternary complex with topotecan (*15*), the drug intercalated as a bp, increasing the distance between the −1 and +1 bp up to 7.2 Å. Several interactions stabilized this conformation, as two water-mediated hydrogen bonds with N722 and the catalytic phosphotyrosine, and there is one direct hydrogen bond between the 20-*S*-hydroxyl residue of topotecan and D533. The TFO−CPT conjugate apparently bypasses this necessary requirement by placing a CPT analogue in the cleavage complex, thus rendering the 20-hydroxyl group an unnecessary structural feature. In fact, our molecular-modeling studies reveal that the 20-*S*-OH makes only a small contribution when CPT is attached to the TFO via the 10 position. Consequently, the 20-deoxyCPT−TFO conjugate maintained DNA-cleaving ability equivalent to the parent conjugate. The importance of the TFO and linker in stabilizing the interactions of CPT with the topo I/DNA active site is emphasized.

This feature of the conjugates may be further exploited to enlarge the family of CPT derivatives that poison topo I and induce DNA damage. When linked appropriately to a TFO, CPT does not need to sample DNA binding sites until it finds a cleavage complex ideal to form a stable ternary complex, because the TFO moiety of the conjugate tightly positions and holds the linked CPT in the topo I/DNA active site.

As for inactive CPT derivatives, it is believed that several topo I mutants are resistant to CPT, because they have mutations near the topo I/DNA active site that remove an amino acid hydrogen bond important for stabilizing the ternary complex, as D533, R364, and N722 (*14*, *17*). Molecular-modeling studies have shown that these topo I mutants do not create a steric clash that would prevent the CPT from docking into the active site of the mutants (data not shown); therefore, *a priori*, the conjugates could still position CPT in the active site. As mutants, we chose mutant R364H, in which a histidine replaces arginine 364, and mutant N722S, in which asparagine 722 is substituted by a serine (Figures 5 and 6 and Table 1). The conjugation of cCPT to the TFO (TFO16−L4−cCPT) did not overcome the resistance, while the MGB−cCPT conjugate did induce some DNA cleavage in the presence of the R364H mutant, thus partly evading resistance to CPT. In the presence of the N722S topo I mutant, no cleavage was observed. These differences in behavior could be explained by the fact that the R364H mutation is adjacent to the minor groove of the DNA, while N722S projects into the major groove (Figure 7B). In the case of 7CPT, the R364H mutant is still poisoned. The TFO16−L6−7CPT conjugate induced significant DNA cleavage in the presence of the R364H mutant and, moreover, formed the ternary complex also in the presence of the N722S mutant. This conjugate allows CPT to make an optimal network of hydrogen-bonds and electrostatic interactions with active-site residues and bases (parts A and B of Figure 7). The amount of cleaved DNA, observed in the presence of the topo I mutants, is small, but it is important to emphasize that the mutant enzymes produce less cleavage on the 324-bp DNA fragment than wild-type topo I (Figure 5). The 20-*S*-hydroxyl was less important for the R364H mutant than for the N722S mutant, as shown by the dCPT derivative alone and conjugated to MGB. Again the TFO conjugate behaved the same as the dCPT alone.

Altogether these findings with different attachment points on the CPT skeleton, linker arms, and DNA ligands indicate that all CPT conjugates can bind to and stabilize the topo I/DNA cleavage complex, confirming that several conformations may coexist in the ternary complex. However, while positions 7, 9, and 10 are favorable to the conjugation, position 12 is completely unfavorable, probably because the linker arm to the TFO moiety clashes with topo I/DNA in the ternary complex. The fact that attachment via position 12 afforded a conjugate incapable of stabilizing DNA cleavage, in parallel with the behavior of free CPT, argues strongly that the activity of the other conjugates probably does reflect binding interactions fundamentally analogous to those accessible to the free CPTs. The molecular-modeling studies presented here in fact support this conclusion, because CPT in the TFO16−L6−7CPT conjugate was able to bind in nearly the identical orientation and with the same network of hydrogen-bond/electrostatic interactions to the topo I/DNA active site, as does free CPT and active derivatives (*14*, *22*).

The use of the conjugates facilitates the understanding of the mode of binding of CPT in the covalent topo I/DNA cleavage complex and the specific roles of the various structural features of CPT. Importantly, the loss of the 20-*S*-OH, a hydrogen-bond donor, in the CPT 20-deoxy derivative, can be compensated for by conjugating it to the TFO, which stabilizes the ternary complex upon triplex formation: the TFO16−L4−dCPT was nearly as active as its 20-*S*-OH analogue, TFO16−L4−cCPT. Furthermore, the conjugates can have other important implications in that they partially overcame the CPT resistance of the topo I resistance mutants N772S and R364H, as is shown by the TFO−7CPT and MGB−cCPT conjugates.

Our present observations underline the structural interactions of the TFO−CPT conjugates in the ternary complex. The ability to effect sequence-specific cleavage of DNA and to stabilize the cleavage product provides a novel and direct strategy for the design of new antitumor agents with increased efficacy and selectivity for specific genes.

REFERENCES

1. Thomas, C. J., Rahier, N. J., and Hecht, S. M. (2004) Camptothecin: Current perspectives, *Bioorg. Med. Chem. 12*, 1585−1604.
2. Champoux, J. J. (2001) DNA topoisomerases: Structure, function, and mechanism, *Annu. Rev. Biochem. 70*, 369−413.
3. Pommier, Y., Redon, C., Rao, V. A., Seiler, J. A., Sordet, O., Takemura, H., Antony, S., Meng, L., Liao, Z., Kohlhagen, G., Zhang, H., and Kohn, K. W. (2003) Repair of and checkpoint response to topoisomerase I-mediated DNA damage, *Mutat. Res. 532*, 173−203.
4. Jaxel, C., Capranico, G., Kerrigan, D., Kohn, K. W., and Pommier, Y. (1991) Effect of local DNA sequence on topoisomerase I cleavage in the presence or absence of camptothecin, *J. Biol. Chem. 266*, 20418−20423.
5. Matteucci, M., Lin, K.-Y., Huang, T., Wagner, R., Sternbach, D. D., Mehrotra, M., and Besterman, J. M. (1997) Sequence-specific targeting of duplex DNA using a camptothecin−triple-helix forming oligonucleotide conjugate and topoisomerase I, *J. Am. Chem. Soc. 119*, 6939−6940.

6. Arimondo, P. B., Bailly, C., Boutorine, A., Ryabinin, V., Syniakov, A., Sun, J. S., Garestier, T., and Helene, C. (2001) Directing topoisomerase I-mediated DNA cleavage to specific sites by camptothecin tethered to minor and major groove ligands, *Angew. Chem., Int. Ed. 40*, 3045−3048.
7. Wang, C. C., and Dervan, P. B. (2001) Sequence-specific trapping of topoisomerase I by DNA binding polyamide−camptothecin conjugates, *J. Am. Chem. Soc. 123*, 8657−8661.
8. Arimondo, P. B., Boutorine, A., Baldeyrou, B., Bailly, C., Kuwahara, M., Hecht, S. M., Sun, J. S., Garestier, T., and Helene, C. (2002) Design and optimization of camptothecin conjugates of triple helix-forming oligonucleotides for sequence-specific DNA cleavage by topoisomerase I, *J. Biol. Chem. 277*, 3132−3140.
9. Arimondo, P. B., Angenault, S., Halby, L., Boutorine, A., Schmidt, F., Monneret, C., Garestier, T., Sun, J. S., Bailly, C., and Helene, C. (2003) Spatial organization of topoisomerase I-mediated DNA cleavage induced by camptothecin−oligonucleotide conjugates, *Nucleic Acids Res. 31*, 4031−4040.
10. Hertzberg, R. P., Caranfa, M. J., and Hecht, S. M. (1989) On the mechanism of topoisomerase I inhibition by camptothecin: Evidence for binding to an enzyme−DNA complex, *Biochemistry 28*, 4629−4638.
11. Jaxel, C., Kohn, K. W., Wani, M. C., Wall, M. E., and Pommier, Y. (1989) Structure−activity study of the actions of camptothecin derivatives on mammalian topoisomerase I: Evidence for a specific receptor site and a relation to antitumor activity, *Cancer Res. 49*, 1465−1469.
12. Kehrer, D. F., Soepenberg, O., Loos, W. J., Verweij, J., and Sparreboom, A. (2001) Modulation of camptothecin analogs in the treatment of cancer: A review, *Anticancer Drugs 12*, 89−105.
13. Kerrigan, J. E., and Pilch, D. S. (2001) A structural model for the ternary cleavable complex formed between human topoisomerase I, DNA, and camptothecin, *Biochemistry 40*, 9792−9798.
14. Laco, G. S., Collins, J. R., Luke, B. T., Kroth, H., Sayer, J. M., Jerina, D. M., and Pommier, Y. (2002) Human topoisomerase I inhibition: Docking camptothecin and derivatives into a structure-based active site model, *Biochemistry 41*, 1428−1435.
15. Staker, B. L., Hjerrild, K., Feese, M. D., Behnke, C. A., Burgin, A. B., Jr., and Stewart, L. (2002) The mechanism of topoisomerase I poisoning by a camptothecin analog, *Proc. Natl. Acad. Sci. U.S.A. 99*, 15387−15392.
16. Pommier, Y., Pourquier, P., Urasaki, Y., Wu, J., and Laco, G. S. (1999) Topoisomerase I inhibitors: Selectivity and cellular resistance, *Drug Resist. Updates 2*, 307−318.
17. Chrencik, J. E., Staker, B. L., Burgin, A. B., Pourquier, P., Pommier, Y., Stewart, L., and Redinbo, M. R. (2004) Mechanisms of camptothecin resistance by human topoisomerase I mutations, *J. Mol. Biol. 339*, 773−784.
18. Cantor, C. R., Warshaw, M. M., and Shapiro, H. (1970) Oligonucleotides interactions. III. Circular dichroism studies of the conformation of deoxyoligonucleotides, *Biopolymers 9*, 1059−1077.
19. Arimondo, P. B., Bailly, C., Boutorine, A., Moreau, P., Prudhomme, M., Sun, J. S., Garestier, T., and Helene, C. (2001) Triple helix-forming oligonucleotides conjugated to indolocarbazole poisons direct topoisomerase I-mediated DNA cleavage to a specific site, *Bioconjugate Chem. 12*, 501−509.
20. Antony, S., Jayaraman, M., Laco, G., Kohlhagen, G., Kohn, K. W., Cushman, M., and Pommier, Y. (2003) Differential induction of topoisomerase I−DNA cleavage complexes by the indenoisoquinoline MJ-III-65 (NSC 706744) and camptothecin: Base sequence analysis and activity against camptothecin-resistant topoisomerases I, *Cancer Res. 63*, 7428−7435.
21. Redinbo, M. R., Stewart, L., Kuhn, P., Champoux, J. J., and Hol, W. G. (1998) Crystal structures of human topoisomerase I in covalent and noncovalent complexes with DNA, *Science 279*, 1504−1513.
22. Laco, G. S., Du, W., Kohlhagen, G., Sayer, J. M., Jerina, D. M., Burke, T. G., Curran, D. P., and Pommier, Y. (2004) Analysis of human topoisomerase I inhibition and interaction with the cleavage site +1 deoxyguanosine, via *in vitro* experiments and molecular modeling studies, *Bioorg. Med. Chem. 12*, 5225−5235.
23. Hertzberg, R. P., Caranfa, M. J., Holden, K. G., Jakas, D. R., Gallagher, G., Mattern, M. R., Mong, S. M., Bartus, J. O., Johnson, R. K., and Kingsbury, W. D. (1989) Modification of the hydroxy lactone ring of camptothecin: Inhibition of mammalian topoisomerase I and biological activity, *J. Med. Chem. 32*, 715−720.
24. Wang, X., Zhou, X., and Hecht, S. M. (1999) Role of the 20-hydroxyl group in camptothecin binding by the topoisomerase I−DNA binary complex, *Biochemistry 38*, 4374−4381.
25. Froehler, B. C., Jones, R. J., Cao, X. D., and Terhorst, T. J. (1993) Oligonucleotides derived from 5-(1-propynyl)-2′-*O*-allyl-uridine and 5-(1-propynyl)-2′-*O*-allyl-cytidine−Synthesis and RNA duplex formation, *Tetrahedron Lett. 34*, 1003−1006.
26. Hsiang, Y. H., Liu, L. F., Wall, M. E., Wani, M. C., Nicholas, A. W., Manikumar, G., Kirschenbaum, S., Silber, R., and Potmesil, M. (1989) DNA topoisomerase I-mediated DNA cleavage and cytotoxicity of camptothecin analogues, *Cancer Res. 49*, 4385−4389.
27. Urasaki, Y., Laco, G. S., Pourquier, P., Takebayashi, Y., Kohlhagen, G., Gioffre, C., Zhang, H., Chatterjee, D., Pantazis, P., and Pommier, Y. (2001) Characterization of a novel topoisomerase I mutation from a camptothecin-resistant human prostate cancer cell line, *Cancer Res. 61*, 1964−1969.
28. Fujimori, A., Harker, W. G., Kohlhagen, G., Hoki, Y., and Pommier, Y. (1995) Mutation at the catalytic site of topoisomerase I in CEM/C2, a human leukemia cell line resistant to camptothecin, *Cancer Res. 55*, 1339−1346.
29. Redinbo, M. R., Champoux, J. J., and Hol, W. G. (2000) Novel insights into catalytic mechanism from a crystal structure of human topoisomerase I in complex with DNA, *Biochemistry 39*, 6832−6840.
30. Yaegashi, T., Sawada, S., Nagata, H., Furata, T., Yokokura, T., and Miyasaka, T. (1994) *Chem. Pharm. Bull. 42*.
31. Wall, M. E., Wani, M. C., Nicholas, A. W., Manikumar, G., Tele, C., Moore, L., Truesdale, A., Leitner, P., and Besterman, J. M. (1993) Plant antitumor agents. 30. Synthesis and structure activity of novel camptothecin analogs, *J. Med. Chem. 36*, 2689−2700.

BI048031K